

713

Institut de Physique Nucléaire de Lyon

Université Claude Bernard

IN2P3 - CNRS



CERN LIBRARIES, GENEVA

SCAN-9806044

swg824

IPNLyon 9802

January 1998

Transverse momentum of $J/\psi, \psi'$ and mass continuum muon
pairs produced in $^{32}\text{S-U}$ collisions at 200 GeV/c per nucleon

NA38 Collaboration

M. Bedjidian, D. Contardo, O. Drapier, J.Y. Grossiord, A. Guichard,
R. Haroutunian, F. Ohlson-Malek, J.R. Pizzi

Submitted to Physics Letters B

Transverse momentum of J/ψ , ψ' and mass continuum muon pairs produced in ^{32}S -U collisions at 200 GeV/c per nucleon

NA38 Collaboration

M.C. Abreu ^{a,1}, J. Astruc ^b, C. Baglin ^c, A. Baldit ^d, M. Bedjidian ^e, P. Bordalo ^{a,2},
A. Borhani ^f, A. Bussière ^c, P. Busson ^f, J. Castor ^d, T. Chambon ^d, C. Charlot ^f,
B. Chaurand ^f, I. Chevrot ^d, D. Contardo ^e, E. Descroix ^{e,3}, A. Devaux ^d, O. Drapier ^e,
B. Espagnon ^d, J. Fargeix ^d, R. Ferreira ^{a,4}, F. Fleuret ^f, P. Force ^d, J. Gago ^a,
C. Gerschel ^b, M. Gonin ^f, P. Gorodetzky ^{g,5}, J.Y. Grossiord ^e, A. Guichard ^{e,9},
J. Guimarães ^{a,6}, J.P. Guillaud ^c, R. Haroutunian ^e, D. Jouan ^b, L. Kluberg ^f,
R. Kossakowski ^c, G. Landaud ^d, D. Lazic ^g, P. Liaud ^c, C. Lourenço ^{a,4}, L. Luquin ^{d,7},
R. Mandry ^e, S. Mourgues ^d, F. Ohlsson-Malek ^{e,8}, S. Papillon ^b, P. Petiau ^f,
J.R. Pizzi ^e, C. Racca ^g, S. Ramos ^{a,2}, A. Romana ^f, B. Ronceux ^c, P. Saturnini ^d,
S. Silva ^a, P. Sonderegger ^h, X. Tarrago ^b, J. Varela ^{a,4}

^a *LIP, Av. E. Garcia, 14-1, P-1000 Lisbon, Portugal*

^b *Institut de Physique Nucléaire, IN2P3-CNRS et Université de Paris-Sud, F-91406 Orsay Cedex, France*

^c *Laboratoire d'Annecy-le-Vieux de Physique des Particules, IN2P3-CNRS, B.P. 110, F-74941 Annecy-le-Vieux Cedex, France*

^d *Laboratoire de Physique Corpusculaire de Clermont-Ferrand IN2P3-CNRS et Université Blaise Pascal, F-63177 Aubière Cedex, France*

^e *Institut de Physique Nucléaire de Lyon IN2P3-CNRS et Université Claude Bernard, 43, B^d du 11 Novembre 1918, F-69622 Villeurbanne Cedex, France.*

^f *Laboratoire de Physique Nucléaire des Hautes Energies, Ecole Polytechnique, IN2P3-CNRS, F - 91128 Palaiseau Cedex, France*

^g *Institut de Recherches Subatomiques, IN2P3-CNRS et Université Louis Pasteur, BP 28, F-67037 Strasbourg Cedex 2, France*

^h *CERN, CH-1211 Geneva 23, Switzerland*

Abstract : We have studied the production of J/ψ , ψ' and prompt muon pairs in the mass continuum from a sample of sulfur-uranium interactions at 200 GeV/c per nucleon. We report, in this letter, results obtained for the transverse momentum distributions and their dependence on the transverse energy released in the collision, used as an estimator of the centrality of the nucleus-nucleus interaction.

PACS numbers : 12.38.Mh, 24.85.+p, 25.75.-q

Keywords : ultrarelativistic heavy-ion collisions, J/ψ , ψ' , muon pairs, transverse momentum.

1 Introduction

Since the initial prediction made by T. Matsui and H. Satz [1], the production of charmonium has been studied extensively in ultrarelativistic nucleus-nucleus reactions as a potential signature of a phase transition of matter, from its ordinary state to the theoretically predicted Quark Gluon Plasma (QGP) phase. In the search for the predicted J/ψ suppression, experiment NA38 has reported results on J/ψ and ψ' production obtained with 200 GeV/c per nucleon incident ^{16}O and ^{32}S ion beams on various targets [2]. Theoretical studies have been extended to the transverse momentum distributions of charmonium states which, according to some authors [3], could help to identify and sign QGP production. First transverse momentum results of experiment NA38 can be found in [4].

We report in this letter the final results obtained by the experiment from high precision measurements in sulfur-uranium interactions. We study the transverse momentum distributions of J/ψ and ψ' and, for comparison purposes, we also consider the muon pairs in the mass continuum. The size of the experimental data sample allows to investigate the dependence of the distributions as a function of the transverse energy of the reaction which is directly related to the centrality of the sulfur-uranium interaction.

2 Apparatus

The data were collected at the CERN SPS with a 200 GeV/c per nucleon sulfur beam and a 12 mm thick segmented uranium target. Muon pairs were detected in the kinematical domain defined by a laboratory rapidity range $2.8 < y_{lab} < 4.1$ and a decay angle in the Collins-Soper frame $-0.5 < \cos \theta_{cs} < 0.5$ [5]. The neutral transverse energy was measured by an electromagnetic calorimeter in the pseudorapidity range $1.7 < \eta < 4.1$. Details on the experimental apparatus and data selection criteria can be found in ref. [6]. The statistics collected amounts to ~ 120000 J/ψ .

The muon pairs detected by the apparatus have invariant masses up to $8 \text{ GeV}/c^2$. In the mass range considered here, i.e. above $1.5 \text{ GeV}/c^2$, they originate from the decay of the J/ψ and ψ' mesons, as well as from the mass continuum which is due to both the Drell-Yan pair production mechanism and to the semi-leptonic decay of charmed mesons from $D\bar{D}$ associated production. All these *signal* contributions lead only to opposite-sign (OS) muon pairs. An additionnal contribution to the muon pair mass continuum is due

¹ Also at FCUL, Universidade de Lisboa, Lisbon, Portugal

² Also at IST, Universidade Técnica de Lisboa, Lisbon, Portugal

³ Now at Université Jean Monnet, Saint-Etienne, France

⁴ Now at CERN, Geneva, Switzerland

⁵ Now at PCC, Collège de France, Paris, France

⁶ Now at Johns Hopkins University, Baltimore, USA

⁷ Now at SUBATECH, Ecole des Mines de Nantes, Nantes, France

⁸ Now at ISN, Grenoble, France

⁹ Corresponding author, Tel: (33) 4 72 44 84 46, Fax: (33) 4 72 44 80 04, guichard@ipnl.in2p3.fr

to *background*. It arises from π and K meson decay and leads to opposite-sign as well as to like-sign (LS) muon pairs. The opposite-sign muon pair mass spectrum of the selected data sample, as measured by the experiment, is shown in Fig. 1.

3 Analysis

The transverse momentum distributions are obtained from the measured data using a 4-dimensional unfolding method [7]. The main advantage of a multidimensional method is that no assumptions have to be made neither on the shape of the different kinematical distributions nor on the nature of the physical processes involved in a particular mass region. Four kinematical variables are used to completely define the dimuon quadrivector, i.e. the mass M , the transverse momentum P_T , the rapidity y_{cm} in the center of mass system and $\cos \theta_{cs}$. Four dimensional acceptance and smearing matrices are determined as follows. For computing practical reasons, the acceptance is calculated on a limited set of nodes and interpolations between these nodes are made where needed. The calculation is based on Monte-Carlo programs [8] which simulate the whole apparatus and uses the standard reconstruction and selection procedures. The smearing matrix depends on 8 variables, which leads to $\simeq 10^{13}$ elements. Again for practical computing reasons, instead of handling directly muon pairs, the dimuon smearing matrix is deduced with the simulation program from a limited sample of *single* muons which are then recombined into pairs. Such an approach is much faster and avoids huge storage of data. Details on the method can be found in [7].

The unfolding procedure is applied only to the *signal* sample of events, after prior subtraction of the *background*. In the OS muon pair sample, the contribution of the background to be subtracted from any considered kinematical cell is given by $2\sqrt{N^{++}N^{--}}$, where N^{++} (N^{--}) is the number of positive (negative) like-sign muon pairs [2,4]. In a multidimensional approach, this usual subtraction procedure can no longer be applied since very often, in a given cell, either N^{++} or N^{--} will be zero. In order to overcome this practical problem arising from the limited size of the background sample of events, the shape of the background is determined using the exhaustive combinatorial method developed in ref. [9]. The combination of each single background muon of a given sign with all the other muons of the other sign allows to build a huge sample of background muon pairs which, appropriately normalized, smoothly populates all the individual cells considered in the analysis. Finally, a smoothing procedure has been developed [7] in order to treat the cells where, due to statistical fluctuations of the signal, the subtraction leads to a negative content.

4 P_T distributions

An unfolded muon pair mass spectrum, without any selection on the transverse energy E_T^0 , is shown in Fig. 2. The width of the J/ψ peak in the deconvoluted spectrum is 66 MeV/c²

to be compared with $147 \text{ MeV}/c^2$ in the original data, which allows an easier separation between J/ψ and ψ' . The unfolded P_T distributions are displayed in Fig. 3 for muon pairs with invariant mass in the ranges $2.1 < M < 2.7 \text{ GeV}/c^2$ (intermediate mass region, IMR), $2.8 < M < 3.4 \text{ GeV}/c^2$ (J/ψ), $3.5 < M < 3.9 \text{ GeV}/c^2$ (ψ') and $M > 4.2 \text{ GeV}/c^2$ (Drell-Yan). In order to correct for muon pairs in the mass continuum which contaminate the resonances mass ranges as defined above, the transverse momentum distribution for the J/ψ (resp. ψ') is obtained after subtraction of the P_T distribution of muon pairs in the IMR mass region (resp. with masses above $4.2 \text{ GeV}/c^2$) normalized according to a phenomenological fit to the deconvoluted mass spectrum, as shown in Fig. 2.

The same analysis has been repeated for the 5 transverse energy bins shown in Table 1. The results obtained for the first and second moments of the transverse momentum distribution, $\langle P_T \rangle$ and $\langle P_T^2 \rangle$, are shown in Table 2 for the two mass continuum regions and in Table 3 for the J/ψ and ψ' . They are plotted in Figs. 4 and 5. Concerning the $\langle P_T^2 \rangle$ values of the J/ψ , the systematic error due to the choice of the continuum mass region (IMR or $M > 4.2 \text{ GeV}/c^2$) taken into account in the subtraction procedure is $0.01 (\text{GeV}/c)^2$. The results reported here are fully compatible with those of ref. [10] based on an independent and significantly smaller data sample which was analyzed with a less elaborated method. As a function of transverse energy, $\langle P_T \rangle$ and $\langle P_T^2 \rangle$ exhibit a clear increase for the J/ψ . A qualitatively similar albeit much milder behaviour is observed for muon pairs in the IMR continuum. The $\langle P_T \rangle$ and $\langle P_T^2 \rangle$ values for ψ' are higher than for J/ψ . However, the available statistics does not allow to deduce a conclusive trend from the results obtained for the ψ' and for muon pairs with masses above $4.2 \text{ GeV}/c^2$.

In the case of S-U collisions, current theoretical models of P_T distributions for J/ψ favour an interpretation based on initial state parton scattering [11–13]. Gavin and Vogt [12] point out that such a model implies a flattening of $\langle P_T^2 \rangle$ as a function of E_T^0 . Kharzeev *et al.* [13] take into account both initial state parton scattering and the absorption of a pre-resonant state before J/ψ formation. The results of their calculations are compared with the data in Fig. 5.

In order to study J/ψ production as a function of transverse momentum, we consider the ratios $R_i(P_T)$ of the P_T distribution obtained in the transverse energy bin $E_{T_i}^0$, and normalized by the number of muon pairs with mass $M > 4.2 \text{ GeV}/c^2$, to the same distribution obtained in the first bin $E_{T_1}^0$. These ratios, plotted in Fig. 6, show that, at low P_T , J/ψ is more and more suppressed when centrality increases. The general tendency of these ratios is to increase with P_T . However, the accuracy of the measurements does not allow a clear-cut conclusion for P_T values above $2.5 \text{ GeV}/c$. Theoretical models predict that J/ψ production at high P_T saturates in the case of QGP formation whereas, in the case of initial state parton multiple scattering models [11], it keeps increasing with centrality. The $R_i(P_T)$ results alone do not allow to select one of the two models but, as seen in Fig. 5, the $\langle P_T^2 \rangle$ values agree well with the initial state interaction description. This is coherent with the present understanding of J/ψ suppression in S-U collisions which does not require the formation of deconfined matter [14].

5 M_T distributions

Finally, for comparison purposes with thermal models [15], we have studied the transverse mass of the produced muon pairs. We show in Fig. 7, for different muon pair mass intervals, the distributions of $M_T - M$ where $M_T = \sqrt{(P_T^2 + M^2)}$. In the case of the J/ψ , the M_T distribution has been fitted with the analytical function $\frac{1}{T} M_T^2 K_1\left(\frac{M_T}{T}\right)$ where K_1 is the modified Bessel function and the "inverse slope" T is linked to the temperature of the system. The mean values of $M_T - M$ obtained from the unfolded distributions and the T values determined from the fit are shown in Table 4 as a function of transverse energy. Both exhibit a similar behaviour.

6 Conclusion

We have studied the transverse momentum distributions of muon pairs in the mass range [2.1, 8 GeV/c²] produced in sulfur-uranium reactions at 200 GeV/c per nucleon. In particular, the transverse momentum of J/ψ and ψ' has been determined as a function of the transverse energy which is used as an estimator of the centrality of the collision. The "inverse slope" parameter T of the J/ψ transverse mass distribution has also been measured as a function of centrality. Models based on parton scattering in the initial state reproduce reasonably well the $\langle P_T^2 \rangle$ values of the J/ψ .

References

- [1] T. Matsui and H. Satz, Phys. Lett. B178 (1986) 416.
- [2] NA38 Collab., C. Baglin *et al.*, Phys. Lett. B220 (1989) 471;
NA38 Collab., C. Baglin *et al.*, Phys. Lett. B255 (1991) 459.
- [3] F. Karsch and R. Petronzio, Phys. Lett. B193 (1987) 105;
M.C. Chu and T. Matsui, Phys. Rev. D37 (1988) 1851;
J.P. Blaizot and J.Y. Ollitrault, Phys. Rev. D39 (1989) 232.
- [4] NA38 Collab., C. Baglin *et al.*, Phys. Lett. B251 (1990) 465;
NA38 Collab., C. Baglin *et al.*, Phys. Lett. B262 (1991) 362.
- [5] J.L. Collins and D.E. Soper, Phys. Rev. D23 (1981) 1070.
- [6] A. Borhani, Thesis, Université Paris 6 (1996).
- [7] NA38 Collab., M.C. Abreu *et al.*, LYCEN 9747,
accepted for publication in Nucl. Inst. Meth. A.
- [8] Dimujet/Dimurec user's guides, NA38/NA50 internal notes.
- [9] S. Papillon, Thesis, Université Paris 7, IPNO T91-03 (1991);
S. Constantinescu, S. Dita and D. Jouan, IPNO DRE 96-01.
- [10] R. Mandry, Thesis, Université de Lyon, LYCEN T 9356 (1993).
- [11] S. Gavin and M. Gyulassy, Phys. Lett. B214 (1988) 241;
J. Hüfner, Y. Kurihara and H.J. Pirner, Phys. Lett. B215 (1988) 218;
J.P. Blaizot and J.Y. Ollitrault, Phys. Lett. B217 (1989) 392.
- [12] S. Gavin and R. Vogt, hep-ph/9610432.
- [13] D. Kharzeev, M. Nardi and H. Satz, Phys. Lett. B405 (1997) 14.
- [14] S. Gavin *et al.*, Z. Phys. C61 (1994) 351;
D. Kharzeev *et al.*, Z. Phys. C74 (1997) 307.
- [15] R. Hagedorn, Riv. Nuovo Cimento 6 (1983) 1.

	E_T^0 range (GeV)	$\langle E_T^0 \rangle$ (GeV)
E_{T1}^0	$13 \leq E_T^0 < 34$	25.4 ± 2.5
E_{T2}^0	$34 \leq E_T^0 < 50$	42.2 ± 3.2
E_{T3}^0	$50 \leq E_T^0 < 64$	57.2 ± 3.7
E_{T4}^0	$64 \leq E_T^0 < 77$	70.6 ± 4.1
E_{T5}^0	$77 \leq E_T^0 < 88$	82.1 ± 4.4

Table 1

Upper and lower limits of the five transverse energy intervals, together with the corresponding mean values.

	$2.1 < M < 2.7 \text{ GeV}/c^2$		$M > 4.2 \text{ GeV}/c^2$	
	$\langle P_T \rangle$	$\langle P_T^2 \rangle$	$\langle P_T \rangle$	$\langle P_T^2 \rangle$
E_{T1}^0	0.87 ± 0.04	1.02 ± 0.06	1.09 ± 0.15	1.69 ± 0.40
E_{T2}^0	0.89 ± 0.04	1.15 ± 0.07	1.07 ± 0.13	1.47 ± 0.22
E_{T3}^0	0.90 ± 0.04	1.09 ± 0.06	0.97 ± 0.12	1.34 ± 0.26
E_{T4}^0	0.92 ± 0.04	1.14 ± 0.06	0.97 ± 0.11	1.29 ± 0.20
E_{T5}^0	0.92 ± 0.04	1.12 ± 0.07	1.15 ± 0.13	1.82 ± 0.28
All E_T^0	0.89 ± 0.02	1.07 ± 0.03	1.02 ± 0.05	1.44 ± 0.11

Table 2

Mean values of P_T (GeV/c) and P_T^2 (GeV/c)² calculated from the P_T distributions of two different mass continuum regions, for the different E_T^0 bins.

	J/ ψ		ψ'	
	$\langle P_T \rangle$	$\langle P_T^2 \rangle$	$\langle P_T \rangle$	$\langle P_T^2 \rangle$
E_{T1}^0	1.11 ± 0.01	1.60 ± 0.03	1.20 ± 0.28	2.33 ± 0.67
E_{T2}^0	1.13 ± 0.01	1.66 ± 0.03	1.24 ± 0.29	2.33 ± 0.68
E_{T3}^0	1.15 ± 0.01	1.72 ± 0.03	1.45 ± 0.36	2.80 ± 0.81
E_{T4}^0	1.18 ± 0.01	1.82 ± 0.03	1.54 ± 0.43	3.35 ± 1.03
E_{T5}^0	1.18 ± 0.02	1.81 ± 0.03	1.13 ± 0.43	2.11 ± 1.00
All E_T^0	1.16 ± 0.01	1.75 ± 0.02	1.21 ± 0.12	2.16 ± 0.29

Table 3

Mean values of P_T (GeV/c) and P_T^2 (GeV/c)² calculated from the J/ ψ and ψ' P_T distributions, for the different E_T^0 bins.

	$\langle M_T - M \rangle$ (MeV/c ²)	T (MeV)	χ^2/ndf
E_{T1}^0	239 ± 4	213 ± 3	1.8
E_{T2}^0	249 ± 4	222 ± 3	1.1
E_{T3}^0	256 ± 4	226 ± 3	3.1
E_{T4}^0	269 ± 4	238 ± 3	3.1
E_{T5}^0	269 ± 4	234 ± 3	2.8
All E_T^0	261 ± 2	232 ± 2	2.7

Table 4

Mean values of $M_T - M$ (MeV/c²) calculated from the J/ψ P_T distributions, for the different E_T^0 bins. The parameter T and χ^2/ndf correspond to a fit with the modified Bessel function (see text).

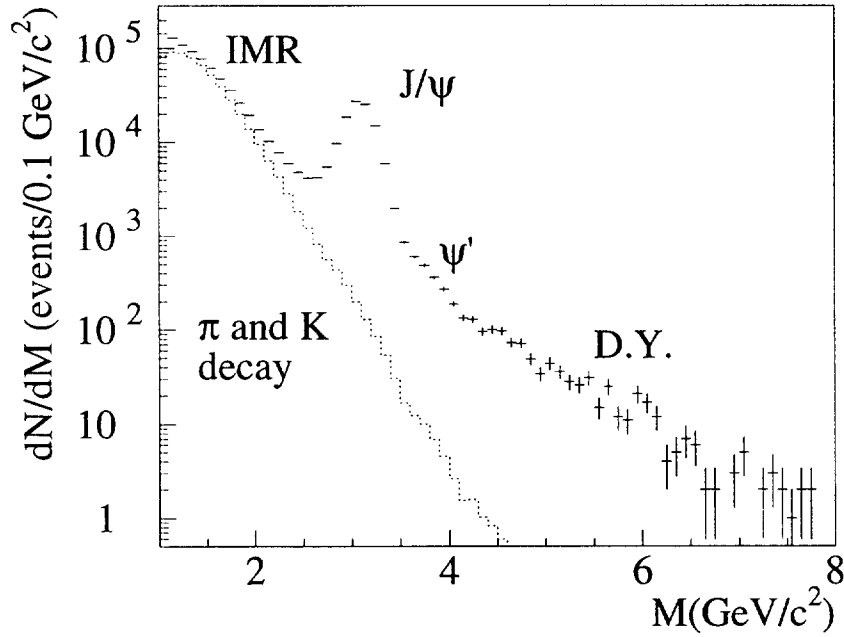


Fig. 1. Opposite-sign muon pair mass distribution. The dotted line stands for the contribution from pion and kaon decay, estimated from the like-sign dimuon mass spectra using the exhaustive combinatorial method (see section 3). IMR stands for the mass region $2.1 < M < 2.7$ GeV/c² (see section 4).

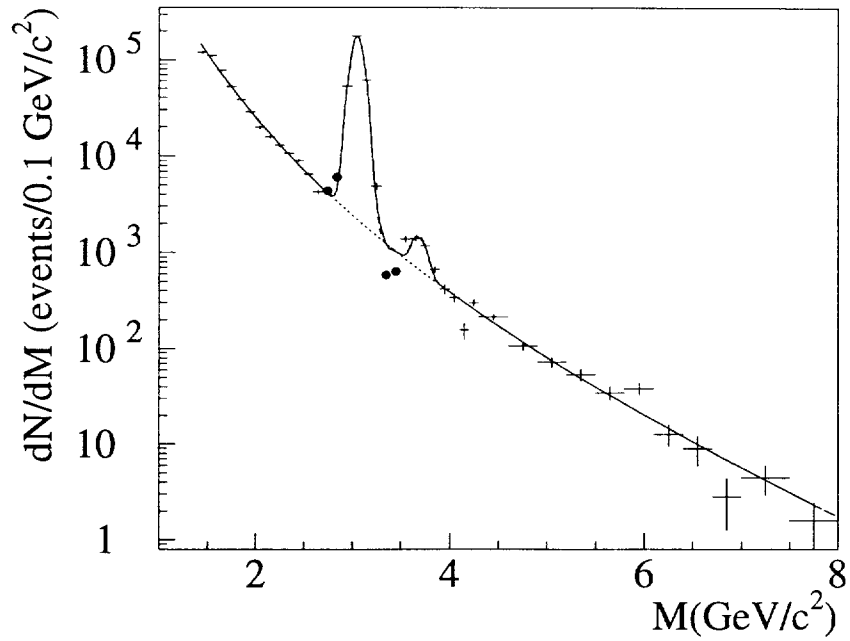


Fig. 2. Deconvoluted mass spectrum. The curve corresponds to a phenomenological fit (see text). The black dots correspond to points removed from the fit.

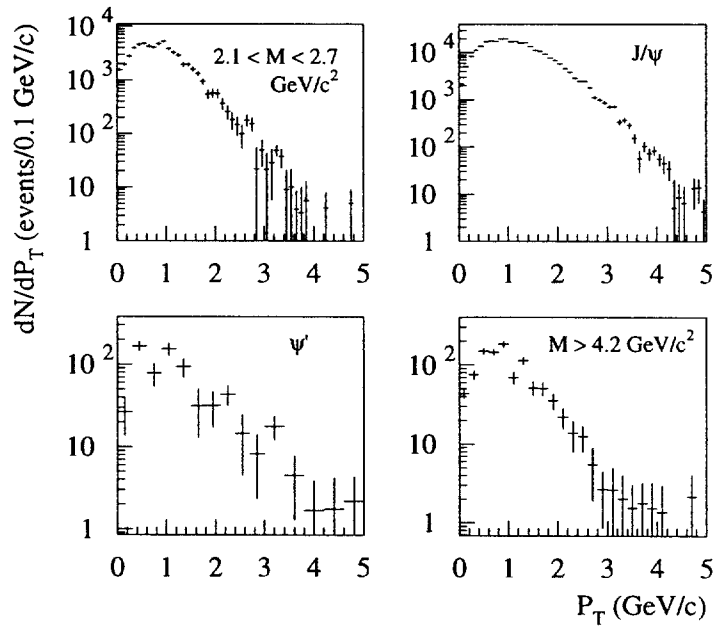


Fig. 3. Unfolded P_T distributions for different muon pair mass intervals.

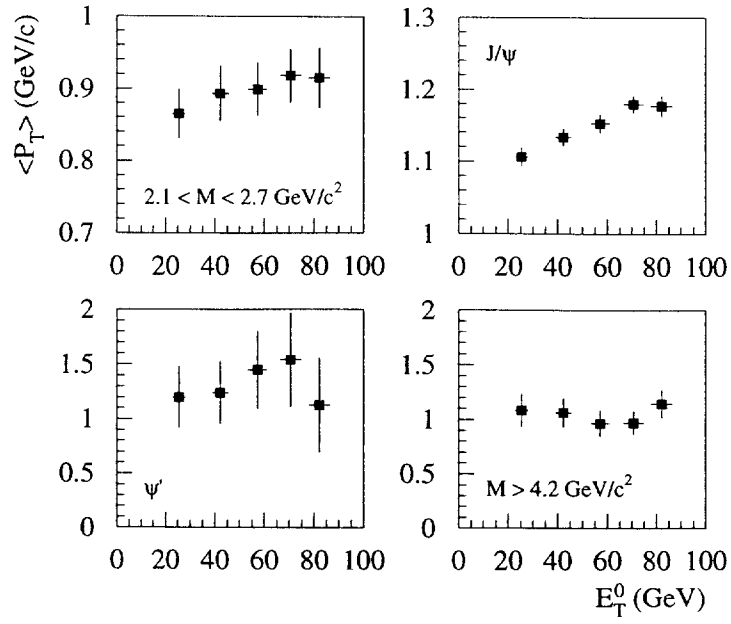


Fig. 4. Distribution of $\langle P_T \rangle$ as a function of the transverse energy for different muon pair mass intervals.

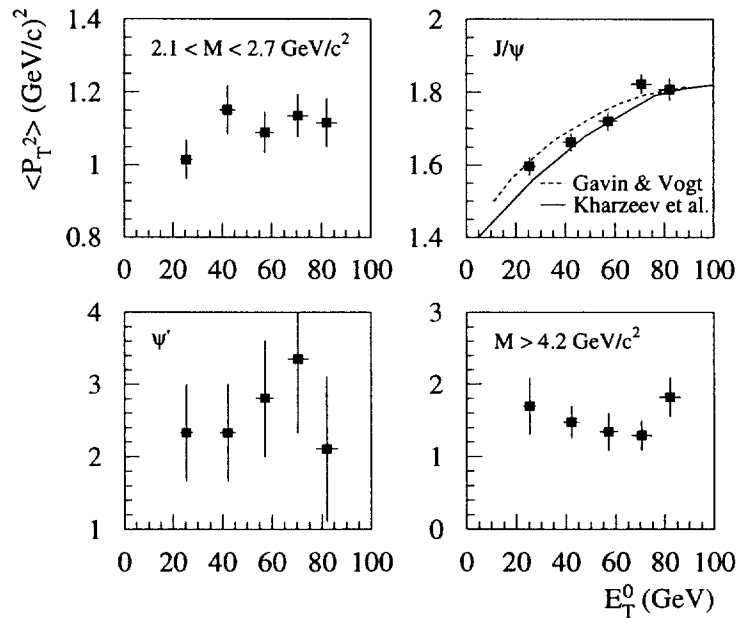


Fig. 5. Distribution of $\langle P_T^2 \rangle$ as a function of the transverse energy for different muon pair mass intervals.

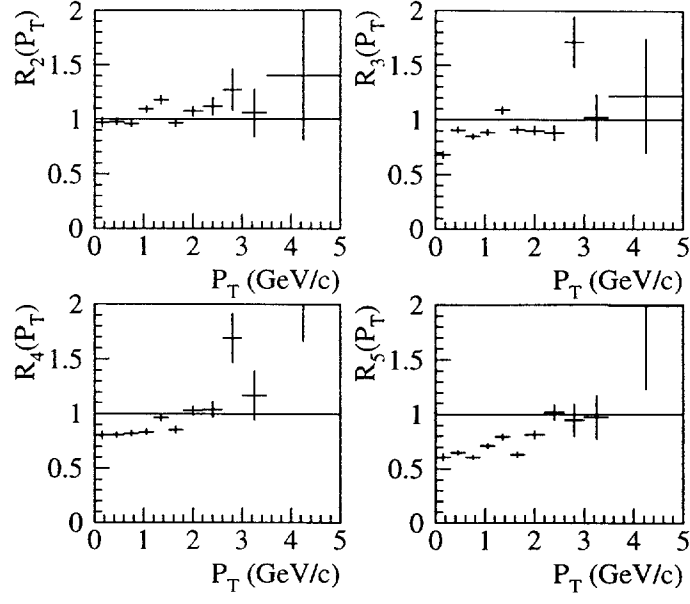


Fig. 6. $R_i(P_T)$ ratios for the J/ψ .

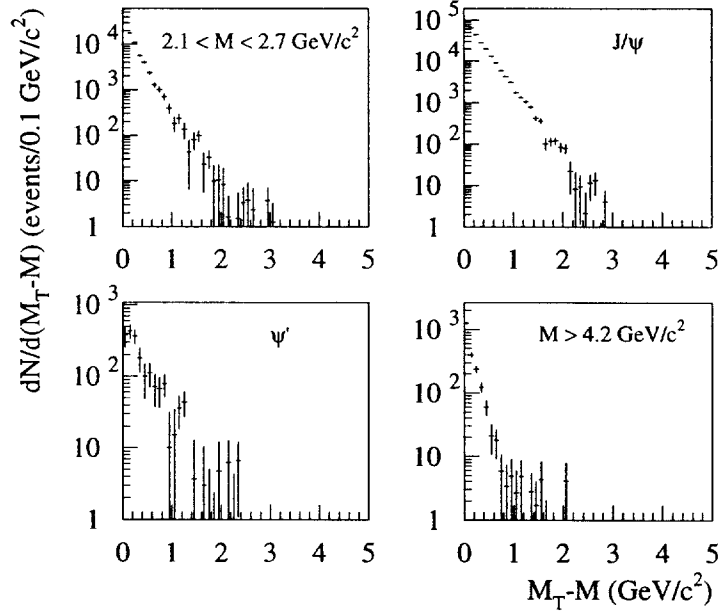


Fig. 7. Unfolded $M_T - M$ distributions for different muon pair mass intervals.

